sciendo

VOLUME 16, Nº 2 2022
Journal of Automation, Mobile Robotics and Intelligent Systems

Vibration Control Using a Modern Control System for Hybrid Composite Flexible Robot Manipulator Arm

Submitted: 3rd February 2022; accepted 12th April 2022

S. Ramalingam, S. Rasool Mohideen

DOI: 10.14313/JAMRIS/2-2022/14

Abstract:
In this research, a model of a robotic manipulator flexible structure and an equation of motion for controller design is planned. The structural material chosen for the robot structure was a hybrid composite. A comparison study was carried out for the aluminium 6082 alloy for the flexible manipulator arm application. Vibration behavior and control implementation was analyzed by adding joint flexibility in the system. Using a simulation algorithm, the system parameter calculation is carried out through MATLAB software for vibration amplitude, transient period, steady-state error, and settling time of flexible robotic arm system. In a systematized motion equation, flexible robotic deflections are organized via the assumed mode (AM) and Lagrange techniques (LT). The graph analysis of hybrid composite and AL6082 materials with high stiffness coefficients is plotted. These obtained values from the plot are utilized for Linear Quadratic Regulator (LQR) controller design. The LQR output facts for both aluminium structural robotic arm and composite material robotic arms are established.

Keywords: *Composite material, Al6082 alloy, Simulation analysis, Vibration amplitude, LQR controller.*

Nomenclatures:

EBBT	–	Euler-Bernoulli Beams Theory
TBT	–	Timoshenko Beam Theory
AMM	–	Assumed Mode Method
FEM	–	Finite Element Method
LPM	–	Lumped Parameter Model
HDPE	–	High Density Polyethylene
MATLAB	–	Math's Laboratory
AL6082	–	Aluminium 6082 alloy
LE	–	Lagrangian Equation
LQR	–	Linear Quadratic Regulator Control
FRP	–	Fiber Reinforced Polymer

1. Introduction

The structural part of the flexible link element of a robotic manipulator with a flexible joint has the ability to reach position accuracy in an obstruction environment of industrial production or fabrication. The flexible material for the robotic link application is an alternative to giant manipulators: that is, a manipulator which has oversize, posture, short range of work envelope with low payload lifting capacity is called a *giant manipulator*. Such a giant manipulator consumes vast energy, requires more task completion time, and has a problematic move-in work envelope. To overcome the issue a flexible material for the robotic link manipulator is introduced. It is lightweight, has less power absorption, has a quick processing time, fewer issues on mass moment inertia, and safe operation for the manipulator.

The main drawbacks encountered in the flexible links are residual vibration in the flexible structure. Kalyoncu [1] devised a revolving prismatic joint attached to the single-link manipulator with sliding robot arm movement and payload at the end portion of the link, an investigation of which leads to the mathematical derivation and the numerical output of a lightweight robot link manipulator with the addition of rotary-prismatic joint movement action.

Ahmad et al. [2] presented a single-link manipulator dynamic analysis which includes damping and hub inertia. The finite element method was used for system performance. Korayem et al. [3] developed modeling of a robotic manipulator with one link for analyses. The impact of beam length and shear deformation is considered using two-beam theories such as Euler-Bernoulli Beams Theory (EBBT) and Timoshenko Beam Theory (TBT). The above methods were established for performance analysis. The EBBT yields good results.

Rishi Raj et al. [4] have discussed the importance of using a digital prototype over a normal prototype for fast-growing industrial automation. At present, the industries are mechanized to meet customer demands and satisfaction. Industrial robots are engaged to perform tasks quickly and accurately. To increase the production rate, lightweight manipulators with composite materials as flexible links are developed. The composite material has the advantage of good mechanical strength, plenty of design option flexibility, comfort in the manufacturing process, good corrosion resistance, impact resistance, and outstanding fatigue strength. Due to the light weight, the moving arms experience very large elastic deformations, and stresses are formed in the loading condition of the manipulator.

The payload and weight of a robotic manipulator ratio for an existing mobile manipulator is starting from 1/10th up to 1/30th. The size of a robotic arm

with the overweight of the end effector of existing industrial robots and their lifting capacity are considered. This ratio is very low when compared to normal human workers: that is, the ratio is 1/3 to 1/5 for an individual person and sometimes more, depending upon the working environment. The increase of manipulator weight takes more time to move from initial point to final position, and the actuator size is also increased. To eliminate the above issue, the first thing is to design changes followed by new materials for robotic arms. A new type of composite material is to be developed and replaced for existing robots as per the normal human capacity ratio of 1/3. This is achieved through lightweight composite material and smart materials for the flexible robotic arm. These lightweight material numerical analysis are required for the standby of rigid and massive robotic manipulators [5]. A literature survey of dynamic modeling of the flexible single arm is discussed and approaches are listed, and also categorized as (a) Assumed Mode (AM) or Shape Function (SF) technique, (b) Finite Element (FE) analysis, (c) Elements of Lumped Mass Models and (d) Other technology studies. A single flexible or AM model with distributed parameters is included in the review robot modeling work by Dwivedy et al., [6-7] and work elaborates the control techniques of joint flexible manipulator robots.

From the information and numerical data collected from research existing work, it is clearly understood that to replace the slow speed robots with higher speed robots one must introduce low density, high mechanical strength arms with homogeneous flexibility. This is a tough task in the field of flexible robotic arm modeling and controls the approach to composite material flexible joint robotic arms. The prime investigation is to compare the steady-state of conventional and composite material flexible robotic arm behaviors.

In this research, to study the model equation of the flexible robotic manipulator arm, the design of a modern controller to reduce vibration and improve performance of a modern controller LQR is to be tested through a simulation tool on a single-link flexible manipulator of both composite and conventional materials. Numerical outputs of hybrid composite and aluminium material robotic arms are to be compared, correlated, and validated**.** The MATLAB software tool is used for simulation output. The graphs were obtained for analysis. The additional goal is to calculate the end effector coordinates of a hybrid composite flexible one-link robotic arm and compare it with the conventional material.

2. Materials and Method

The flexible material and its properties are significant for robotic link applications. The analysis of material suitability for the manipulator's arm is inevitable for replacement giant robotic arms. The reduction of weight and mechanical properties are examined for robotic link material selection. At present, for robotic chasing, a high-density polyethylene (HDPE) material is used which is not suitable for high-temperature environmental conditions and high payload carry tasks. The alternate is aluminum: it has light weight and is corrosion-resistant. But aluminium creates vibration when in operating conditions. Therefore, another alternate solution is to introduce new soft materials as a link as they have the benefit of higher speed, increased area mobility, more efficiency in terms of less energy consumption, and high payload carrying capacity. The use of composite material for a robot manipulator has good mechanical properties, combining two or more fiber materials. It aims to achieve the chosen physical properties, design flexibility, ease of fabrication, light weight, corrosion resistance, impact-resistance, excellent fatigue strength [8], and other desirable characteristics. The applications of robot links are a concern; varieties of fiber materials are used as links, such as carbon material fiber, boron material fiber, ceramic, glass fiber, and aramid fibers.

The robotic link parameters of aluminiun 6082 alloy material and composite material are calculated and listed in Table1. The composite lightweight material is made up of carbon, fiberglass fiber, and Kevlar fiber [9]. Using volume and weight ratio relation, the weight of material and thickness of composite materials are determined. The composite material is taken for simulation study and their parameters are given in Table 1. Both the materials were considered for the same cross-sectional area (A) and length (L) for parameter calculation to analyze the behavior of the materials. The link has also varied the mass as per material density concerned for same length.

Table 1. Materials parameter for aluminium and hybrid composite

Link Parameter	Parameter Symbol	Units	Conventional Material	Hybrid Composite Material
			Aluminium	Carbon + E Glass + Graphite Particulate+ Epoxy
Length of link	L	(m)	1	1
Width of link	d	(m)	0.05	0.05
Thickness of link	t	(m)	0.002	0.002
Cross sectional area	A	(m^2)	0.0001	0.0001
Damping coefficient	ζ	-	0.015	0.015
Mass density	ρ	(kg/m)	0.277	0.09455
Young's modulus	E	(N/m^2)	7e10	4.4942e-3
Area moment of inertia	I	(m^4)	0.33e-10	0.33e-10
Mass of payload	M_p	(Kg)	0.277	0.09455
Inertia without pay load	I_T	(Kgm^2)	0.5	0.4
Inertia with payload	I_T	(Kgm^2)	0.8	0.6
Input torque	$\tau(t)$	(Nm)	1	1

2.1 Robot Arm Kinematics

Robotic arm kinematics deals with the analytical study of the motion of a robot arm w.r.t a fixed reference coordinate system as a function of time. Without regard to the forces or moments that cause the motion. The dynamics robotic arm deals the relation between robot arm motion and forces and moments acting on the robot. The system has pinned-free flexible link as a two degree of freedom (Dof) model.

2.2 Mathematical Modeling

The composite material manipulator as well as the aluminium 6082 alloy material links are considered

as the pinned-free flexible link as a 2Dof model, attached with the circular hub. The circular disc-type hub is moulded with the shaft of a rotating actuator. The rotating robotic link is a bend in a curved form freely in the two-dimensional horizontal plane due to flexibility, but rigid in a vertical position and also in torsion. The robotic arm length, width, and thickness of flexible links are hypothetical to be constant for both materials. The density of both the materials is varying. The robotic arm deformation due to shear as well as inertia due to revolving of the link is neglected as per the TBT theory [10]. The methodology flow chart is shown in Fig. 1. The schematic diagram of a robotic manipulator arrangement is given in Fig. 2.

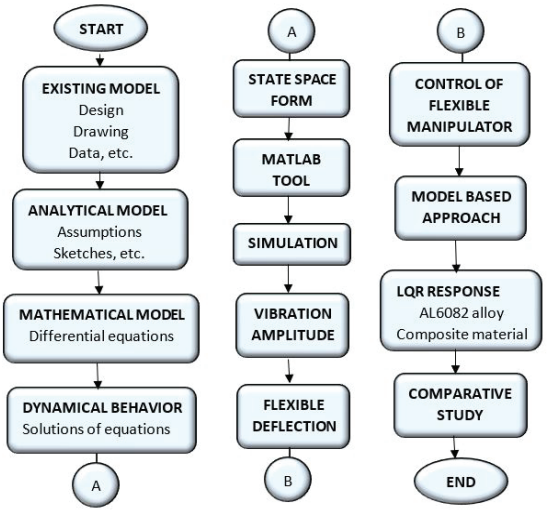

Fig. 1. Model and methodology

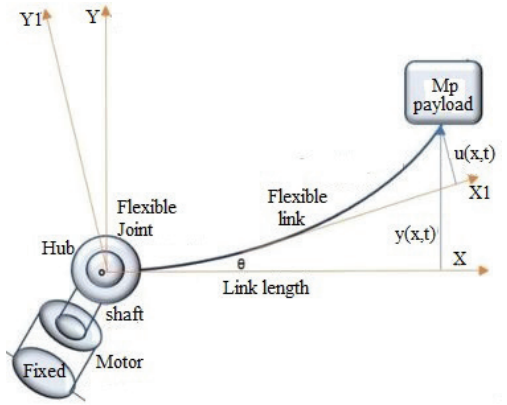

Fig. 2. Composite material flexible link

The payload is attached at the tip of the robotic link and input torque force is given to the rotary hub of the link by an actuator. The 'θ (t)' is angular displacement and 'u (x, t)' is the flexible deflection of the link. Finally, the total displacement of link 'y (x, t)' is calculated. It has two functions: rigid-body rotation 'θ (t)' and link curved deflection 'u (x, t)' given in eq. (1),

$$y(x,t) = u(x,t) + x\theta(t) \tag{1}$$

2. 3 Dynamic Equations

To find the equations of motion of link, initially, the energies connected with systems are calculated. These are kinetic energy (KE), potential energy (PE), and dissipated energies [11]. The kinetic energy of the rotary hub, flexible arm, and tip-attached payload is calculated by considering small curved deflection and small angular velocity. The actuator input force τ (t) is used to calculate the nonconservative work (W) of a system, as

$$W = \tau_m \theta \tag{2}$$

The extended Hamilton's principle is adopted. In this equation, only two modes have been taken for modeling by null rotary inertia and null shear deformation (Meirovitch, 1970). [12] To substitute the value u (x, t) in equation (1) and after simplifying, the motion equation of flexible manipulator with corresponding initial and boundary conditions are given by,

$$EI\frac{\partial^4 y(x,t)}{\partial x^4} + \rho\frac{\partial^2 y(x,t)}{\partial t^2} = 0 \tag{3}$$

where (EI) and (ρ) are the rigidity and density of the link material. The equation (3) is the "fourth-order partial differential equation" (PDE) which gives the motion equation of a flexible robotic arm dynamic model.

2.4 Shape Function

The solution of y (x, t) in the dynamic model of an equation of motion of manipulator as per of assumed mode method is given as,

$$y(x,t) = \sum_{i=1}^{n} \phi_i(x) q_i(t) \tag{4}$$

where, i = 1, 2, ...n, and y *(x, t)* is the total deflection. The displacement $\boldsymbol{\phi}(x)$ along the length of the robotic manipulator is called *mode shape* or *shape function* and $q_i(t)$ is time arbitrary constant. It is derived by taking the *y (x, t)* value from equation (4) and substituting it in equation (1). After mathematical manipulation, it gives two expressions of order, ordinary differential equations. The first 4th order equation is given as,

$$\frac{d^4\phi_i(x,t)}{dx^4} + \beta_i^4\phi_i(x) = 0 \tag{5}$$

Where β_i is constant. For simplification the following quantities are used in the equations for numerical analysis,

$$\beta^4 = \left(\frac{\rho}{EI}\right)^2, \lambda = \beta L, I_b = \frac{\rho L^3}{3}, \varepsilon = \frac{I_h}{3I_b}, \eta = \frac{M_p L^2}{3I_b}, K_c = K_t\frac{EI}{L} \tag{6}$$

where (λ) is system parameter, (I_h) and (I_b) are the hub inertia and link inertia of the system. (k_c) is joint stiffness coefficient, (M) is mass of the manipulator link and 'ε' is the ratio between the hub and link in-

ertias which determines the vibration frequencies of the manipulator. The 'η' represents the ratio between payload inertia and link inertia, which is also indicative of vibration frequencies of the flexible manipulator. The equation (5) is fourth order ODE which has a general solution in the form (Ramalingam et al., 2019) as given below,

$$\phi_i(x) = A_i \sin \beta_i x + B_i \sinh \beta_i x + C_i \cos \beta_i x + D_i \cosh \beta_i x \quad (7)$$

1.5 Natural Frequency

To calculate the natural frequency and mode shape, the λi value satisfies the boundary conditions (*BC*) of the undriven flexible link manipulator. The above quantities are determined with corresponding coefficient values *Ai, Bi, Ci,* and *Di* from equation (7) using orthogonality property and boundary conditions of the systems.

1.6 State Space Model

The derived equations of motion based on the Lagrange principle are transformed in a state-space form [13-14] and [15] and the output as given in matrix form using state-space model as $X^{\bullet} = AX + Bu$ and output as $y = CX$ + D. The matrixes *A, B, C* and *D* are given below as,

$$\begin{bmatrix} q_o' \\ q_o'' \\ q_1' \\ q_1'' \\ q_2' \\ q_2'' \end{bmatrix} = \begin{bmatrix} 0 & 1 & 0 & 0 & 0 & 0 \\ 0 & 0 & 0 & 0 & 0 & 0 \\ 0 & 0 & 0 & 1 & 0 & 0 \\ 0 & 0 & -\omega_1^2 & -2\xi_1\omega_1 & 0 & 0 \\ 0 & 0 & 0 & 0 & 0 & 1 \\ 0 & 0 & 0 & 0 & -\omega_2^2 & -2\xi_2\omega_2 \end{bmatrix} \begin{bmatrix} q_o \\ q_o^{\bullet} \\ q_1 \\ q_1^{\bullet} \\ q_2 \\ q_2^{\bullet} \end{bmatrix} + \begin{bmatrix} 0 \\ 1 \\ 0 \\ \frac{1}{I_T}\frac{d}{dx}\phi_1(0) \\ 0 \\ \frac{d}{dx}\phi_2(0) \end{bmatrix} \tau \quad (8)$$

$$[C] = \begin{bmatrix} 1 & 0 & \frac{d^2\phi_1(L)}{dx^2} & 0 & \frac{d^2\phi_2(L)}{dx^2} & 0 \\ 1 & 0 & \frac{d\phi_1(0)}{dx} & 0 & \frac{d\phi_2(0)}{dx} & 0 \\ 0 & 1 & 0 & \frac{d\phi_1(0)}{dx} & 0 & \frac{d\phi_2(0)}{dx} \end{bmatrix}, [X] = \begin{bmatrix} q_o \\ q_o^{\bullet} \\ q_1 \\ q_1^{\bullet} \\ q_2 \\ q_2^{\bullet} \end{bmatrix}, u = \begin{bmatrix} 0 \\ 1 \\ 0 \\ 1 \\ 0 \\ 1 \end{bmatrix} \tau \quad [D] = [0], \quad (9)$$

2.7 Conventional Material: (Aluminium 6082 alloy)

The AL 6082 alloy material is considered as case-1 for robotic structural study. It is generally used as a structural component and the same is used for robotic flexible structure software simulation.

2.8 System Mode Parameters (λ_i)

The general system characteristic equation is used to find the parameter λi ($i = 0$ *to* 4) for 1st mode, 2nd mode, and 3rd mode vibration frequencies, damped natural frequencies, mode shape constants, mode shape, tip position, deflection for conventional material aluminium for further analysis. The rigid and flexible joint system mode values λ_0 to λ_3 and λ_4 for the payload case and the no-load case is calculated. The values are listed in Table 2. It is observed from Table 2 that the rigid mode is absent for the payload and no-load case of a flexible system.

Table 2. Rigid and flexible joint system mode values Payload case

ε	η	Kc	Modes				
			λ_0	λ_1	λ_2	λ_3	λ_4
0.05	1	0	0	2.6303	4.3386	7.1904	10.2753
		1	-	0.8657	2.7899	4.3563	7.1909
		5	-	1.1009	3.2175	4.4409	7.1927

Table 3. Rigid and flexible joint system mode values No-Payload case

ε	η	Kc	Modes				
			λ_0	λ_1	λ_2	λ_3	λ_4
0.05	0	0	0	2.9673	4.8972	7.8970	11.0107
		1	-	1.2185	3.0902	4.9046	7.8972
		5	-	1.6037	3.4860	4.9392	7.8982

2.9 System Frequencies (AL6082 alloy)

The 'λi' values from Table 2 are used to calculate the natural frequency and damped natural frequency of the aluminium 6082 alloy robotic manipulator system. The obtained frequencies are shown in Table 4 and also noticed from the table that the frequencies are increased due to high flexibility in the joint. The damped natural frequencies are shown in Table 5.

Table 4. Flexible joint system frequencies values for Al 6082 alloys link

ε	η	Kc	Natural Frequencies				
			ω_0	ω_1	ω_2	ω_3	ω_4
0.05	1	0	-	6.3788	17.3552	47.6692	-
		1	-	0.6910	7.1764	17.4971	47.6745
		5	-	1.1164	9.5448	18.1833	47.6997

Table 5. Flexible joint system damped natural frequencies values for Al 6082 alloys link

ε	η	Kc	Damped natural Frequency				
			ω_{d0}	ω_{d1}	ω_{d2}	ω_{d3}	ω_{d4}
0.05	1	0	-	6.3781	17.3533	47.6638	-
		1	-	0.6909	7.1756	17.4952	47.6691
		5	-	1.1163	9.5438	18.1813	47.6943

1.10 Composite Material Parameters

The general characteristic equation of a single-arm robotic manipulator system is resolved for (λ). The obtained values of (λ) are shown in Table 2, which are used for calculating the first mode, second mode, third mode, and fourth mode. The frequency and damped natural frequencies are determined using (λ) values from Table 2. Table 6 and Table 7 show the frequencies and damped natural frequencies for a hybrid composite material system.

Table 6. Flexible joint system frequencies for composite material link

ε	η	Kc	Natural Frequencies				
			ω_0	ω_1	ω_2	ω_3	ω_4
0.05	1	0	-	2.7658e-06	7.5249e-06	2.0669e-05	-
		1	-	2.9960e-07	3.1116e-06	7.5865e-06	2.0671e-05
		5	-	4.8451e-07	4.1385e-06	7.8840e-06	2.0682e-05

Table 7. Flexible joint system damped natural frequencies for composite material link

ε	η	K_c	Damped natural Frequencies				
			ω_{d0}	ω_{d1}	ω_{d2}	ω_{d3}	ω_{d4}
0.05	1	0	-	2.7654e-06	7.5241e-06	2.0666e-05	-
		1	-	2.9956e-07	3.1112e-06	7.5856e-06	2.0668e-05
		5	-	4.8445e-07	4.1380e-06	7.8831e-06	2.0679e-05

1.11 System mode shape constants

The system mode shape constants are calculated using (λi) values for rigid, flexible, and high flexibility joint manipulators. To find *Ai, Bi, Ci* from the above equation (7) by assuming *Di =1*, the calculated values are shown in Table 8. These constants are used for both cases of conventional and hybrid composite materials.

Table 8. Flexible joint system mode shape constants 'λ_i' (*i = 0 to 4*)

ε	η	K_c	Mode shape Constants				
			λ_i	A_i	B_i	C_i	D_i (Assumed)
0.05	1	0	2.6303	-0.8150	0.7914	0.8150	1
			4.3386	1.9474	-1.9538	-1.9474	
		1	0.8657	0.4591	-0.1822	- 0.4591	
			2.7899	-0.5611	0.5429	0.5611	
		5	1.1005	0.8193	- 0.6340	- 0.8193	
			3.2175	-0.0584	0.0478	0.0584	

3. Result and Discussions

The step input signal is given to the aluminium 6082 alloy robotic link manipulator and simulation results for three cases as rigid joint (k_c = 0), flexible joint (k_c = 1), and more flexible joint (k_c = 5) are obtained [16]. The output graphs of aluminium alloy 6082 are given in Figs. 3–13.

3.1 Graphs and Analysis (Al 6082 alloy)

The amplitudes of varying joint stiffness coefficient plots are shown in Figs. 3–6. The amplitudes of the highly flexible joint case of the first mode are 0.355m, the second mode is 0.495m. The system mode shapes are shown in Figs.7–8 and also observed from the plots that the node points are increased by increasing the mode shapes. Fig. 9 gives the maximum deflection of the aluminium link manipulator: the value is 0.456 m noticed from the plot when the stiffness is constant. The tip position of the flexible system measured from the initial coordinate of the system is shown in Fig. 11. The hub angle rotations of the system are shown in Fig. 12. The flexibility shown in Fig. 13.

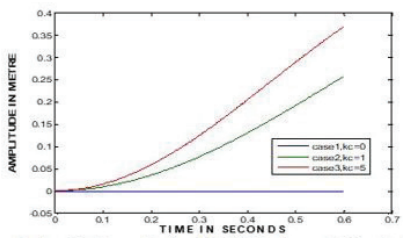

Case 1: λ_0=0, Case 2: λ_1=0.8657, Case.3: λ_1=1.1009

Fig. 3. First mode for three cases of flexible links

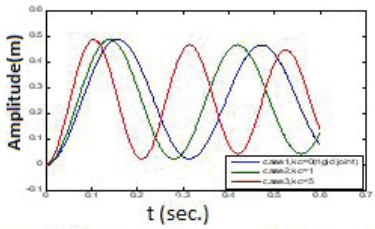

Case 1: λ_1=2.6303, Case 2: λ_2=2.7899, Case.3: λ_2=3.2175

Fig. 4. Second mode for three cases of flexible links

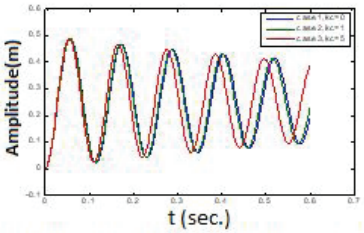

Case 1: λ_2 = 4.3385, Case 2: λ_3=4.3562, Case.3: λ_3=4.4409

Fig. 5. Third mode for three cases of flexible links

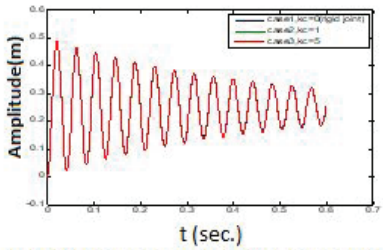

Case 1: λ_3=7.1904, Case 2 λ_4=7.1909, Case 3: λ_4=7.1927

Fig. 6. Fourth mode for three cases of flexible links

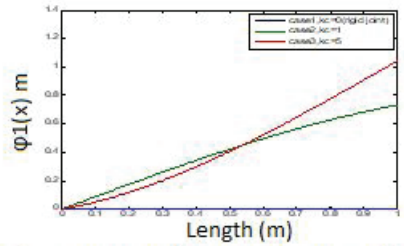

Case 1: λ_0=0, Case 2: λ_1=0.8657, Case.3: λ_1=1.1009

Fig. 7. First mode shape for three cases

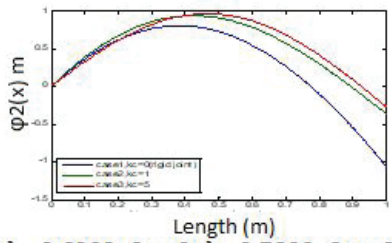

Case1: λ_1=2.6303, Case2: λ_2=2.7899, Case.3: λ_2=3.2175

Fig. 8. Second mode shape for three cases

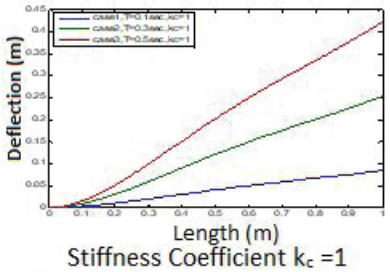

Fig. 9. Deflection of three flexible links

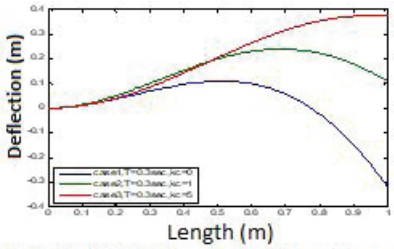

Fig. 10. Deflection of three flexible links

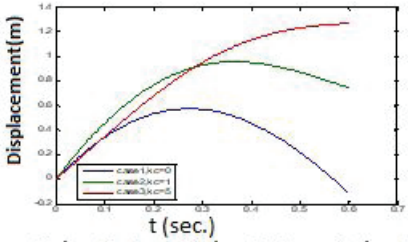

Fig. 11. Tip position (initial co-ordinate)

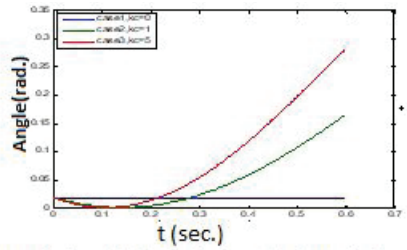

Fig. 12. Angle for three flexible links in radian

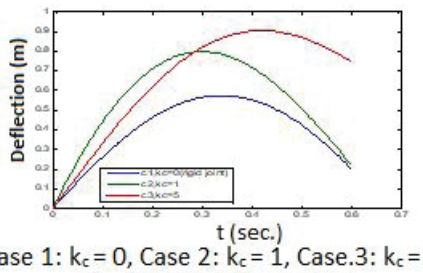

Fig. 13. Flexible deflection

3.2 Graphs and analysis for hybrid composite

The step input signal is given to the hybrid composite manipulator system and simulation output for three cases such as rigid joint (kc = 0), flexible joint, and highly flexible joint (kc = 5) are plotted. The output graphs are shown in Figs. 14–24. The numerical values for the composite material flexible links with different joint flexibilities are calculated.

The amplitude of highly flexible joints for composite material as a case for the first mode is noted as $4x10^{-14}$ m. The system mode shapes are shown in Figs.14–17 and also observed from the plots (Figs. 14–17) that the single node point is obtained by increasing the mode shapes.

Figs.18–19 gives the maximum deflection of composite link manipulator, and value is 0.46 m noticed from the plot when the stiffness is constant. The position of the end link of a system is measured from the fixed coordinate as shown in Fig. 22. The hub angle rotations of the system are shown in Fig. 23.

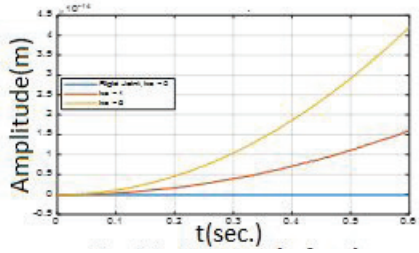

Fig. 14. First mode for three cases of flexible links

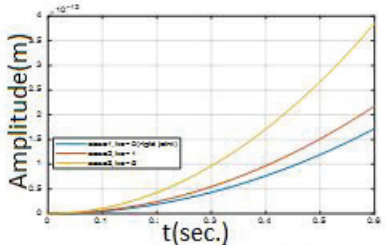

Fig. 15. Second mode for three cases of flexible link

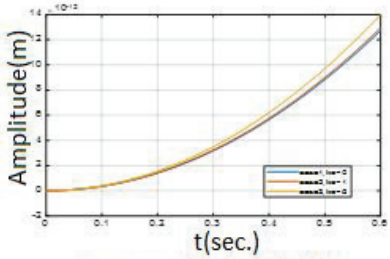

Fig. 16. Third mode for three cases of flexible link

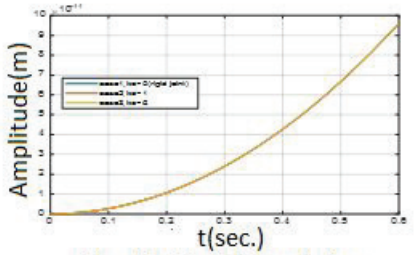

Fig. 17. Fourth mode for three cases of flexible link

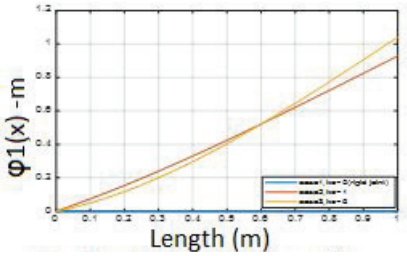

Fig. 18. First mode shape for three cases

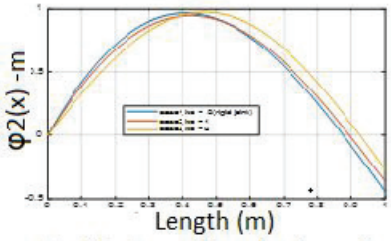

Fig. 19. Second mode shape for three cases

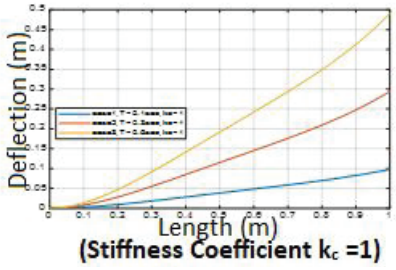

Fig. 20. Deflection of three flexible links

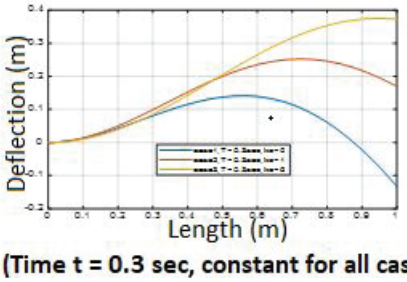

Fig. 21. Deflection of three flexible links

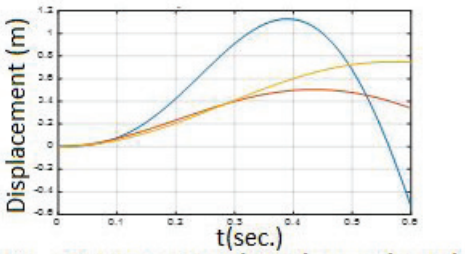

Fig. 22. Tip position (initial co-ordinate) for three flexible links

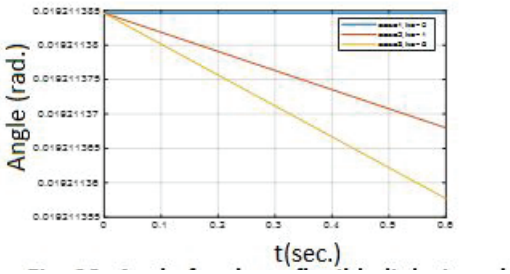

Fig. 23. Angle for three flexible links in rad.

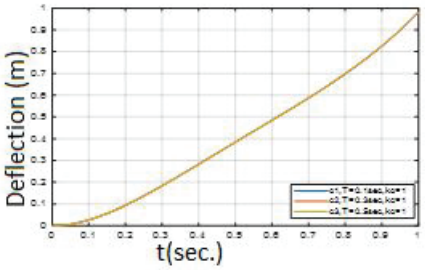

Fig. 24. Tip deflection for three flexible links

3.3 LQR Output Response

The proposed modern control system is activated and simulated through MATLAB, and consists of aluminium alloy robotic arm. Outcomes are shown in Fig. 25.

3.3.1 Aluminium 6082 alloy

The input signal is given to the aluminium alloy 6082 structural robotic manipulators; the output response of the LQR control system [17–18], and [19] are observed. The hub angle and link deflection are not smooth at 0.6 sec. and velocity and acceleration also vary in the system up to a time period of 0.6 sec.

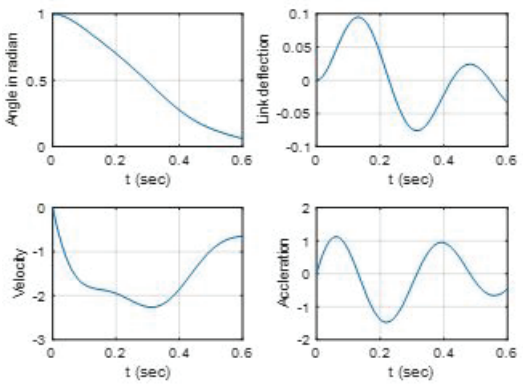

Fig. 25. Optimal quadratic regulator (Step response up to 0.6 seconds)

3.3.2 Composite Material

The modern controller technique of LQR used in the system and unit input torque to the controller. This is applied and simulation is carried out through appropriate software tools [20]. The output plot is shown in Fig. 26. The control scheme characteristic performance calculation of the hybrid composite material is interpolated. The hub angle rotation is settled smoothly at 0.4 sec and flexible arm deflection is a maximum of 0.15 m observed and settled at 0.6 sec. The system hub velocity varies initially and settles at 0.6 sec. Link velocity of the composite material is settled to the setpoint quickly without overshoot up to time t = 0.6 sec. This is shown in Fig. 21b. The output responses of LQR compared to other controllers yields better results in settling time: 0.1sec, steady-state error is 0.31% and the maximum overshoot is 5%.

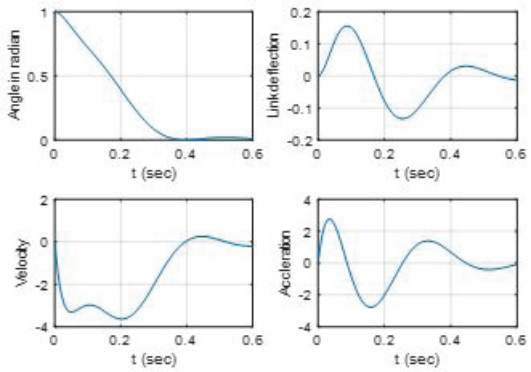

Fig. 26. Optimal quadratic regulator (Step response up to 0.6seconds)

3.4 Comparative Analysis

The common mathematical equation for flexible robot manipulator was derived. This was commonly used for conventional material Al6082 alloy and hybrid polymer composite flexible link manipulators based on the AM method, Hamilton principle, using Lagrange presented. In case-1, analysis was conducted for aluminium alloy (Al6082) and in case-2 analysis for hybrid polymer composite material was done. By considering these materials, the state space solution was obtained.

The composite material single link robot manipulator was used for simulation analysis. It was observed that the composite material link, soft and lightweight, took less power utilization. This was shown in Table 1. The dynamic responses of the flexible manipulators, such as natural frequencies, damped natural frequencies, are calculated as shown in Table 4 to Table 7 and tip deflection for conventional and composite materials has been carried out with flexibility conditions. The results are shown.

The vibration analysis of the system through MATLAB simulation has been conducted by using conventional and hybrid composite laminates; system output is shown in Table 4 and Table 6. The single-link manipulator under step input torque is simulated. The model numerical analysis of the robotic arm is carried out for different joint stiffness coefficients. In addition, lightweight hybrid composite has a quick response while in operating conditions. The materials such as aluminum and hybrid composite are analyzed. This analysis shows the total displacement history and variation of the hub rotation angle of the lightweight hybrid composite robotic link, which is less than that of aluminum materials. The hub angle for the composite link flexible robot manipulator is settled at 0.4 sec. But the 6082-aluminium alloy takes a long time to settle: more than 0.6 sec. The deflection of a lightweight composite material robotic arm is settled without any difficulty at 0.6 sec. But in the case of aluminium 6082 alloy there delay in settling. The velocity of a deflected link at 1.2 sec is smooth. But in the case of aluminium this varies at 0.6 seconds.

3.5 Controller Output Response (Correlation analysis)

The researchers, Hafiz Muhammad Wahaj Aziz, et al. [21] investigated different control systems. The output values of the first-order controller and a super twisting side mode (SMC) controller was listed in Table 9.

Table 9. Output response for first order and super twisting SMC

Step Input	Fist order side mode controller	Super twisting side mode controller
Rise (t_r) time	0.29	0.12
Settling (t_s) time	0.48	0.21
Over (M_p) shoot	0	0
Peak (t_p) time	1.6743	1.1375

The researchers, Waqar Alam et al., [22] were studied using the PID controller and the output responses controller as shown in Fig. 27. From the figure, it is observed that the system settled at desired output with a delay of 0.4363 seconds along with the settling period of time 2 sec.

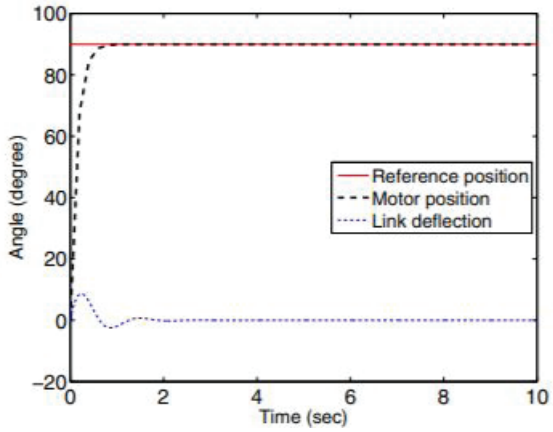

Fig. 27. Lightweight robotic arm trajectory tracking simulation output

The classic PID and modern controllers such as State Feedback and LQR were used in the system by adding step input to the controllers, and output responses are given in Table 10. From this Table 10, the LQR controller yields good results without overshooting. The settling time for the system is noted as 0.1sec.

Table 10. Output response of the PID, SFB and LQR

Step	PID controller	State feedback controller	LQR Controller
settling time (sec.)	48	2.5	0.1
steady state error	-	1.1%	0.31%
percentage of maximum overshoot	35%	10%	5%

By connecting the earlier author's work, namely Hafiz Muhammad Wahaj Aziz, et al. (2016) and Waqar Alam, et al. (2018, results observed from the LQR controller simulation are found to be better.

4. Conclusion

The LQR control system is implemented to control vibration for the composite material link and AL6082 alloy link and compared. It is observed that the total deflection of the composite flexible link is reduced by 41%. But the oscillatory behavior is amplified to 40% higher than the conventional robotic arm. To suppress the vibration amplitude, a controller design is a must for composite material robotic arms. The arm endpoint elastic deflection for the hybrid composite material link is achieved at 5% less. The simulation output of LQR yields better results in settling time: 0.1sec. The steady-state error is 0.31% and the maximum overshoot of 5% is determined. The experimental development for validation of the system is in progress.

Acknowledgment

The authors wish to thank the B. S. A. Crescent Institute of Science and Technology, India, Chennai, which supported us to carry out the work under the No. 2021PDF04.

AUTHORS

S. Ramalingam – AMET University, Department of Mechanical Engineering, Chennai, India,
email: sengalaniramalingam@gmail.com.

S. Rasool Mohideen* – School of Mechanical Science, BSA Crescent Institute of Science and Technology, Chennai, India-48,
email: dean.sms@crescent.education.

* Corresponding author

REFERENCES

[1] M. Kalyoncu, "Mathematical modeling and dynamic response of a multi straight-line path tracing flexible robot manipulator with rotating-prismatic joint", *Applied mathematical modeling*, vol. 32, no. 6, 2008, pp. 1087–98. DOI: 10.1016/j.apm.2007.02.032

[2] M. A Ahmad, M. A Zawawi, "Effect of beam's length on the dynamic modeling of flexible manipulator system", 11th International Conference on Computer Modeling and Simulation, IEEE, 2009, pp. 356–61. DOI: 10.1109/UKSIM.2009.59

[3] M. H. Korayam, A. M. Shafei, S. F. Dehkordi, "Dynamic effect of beam's length and beam's theory on the flexible manipulator system", *International Research Journal of Applied and Basic Sciences*, vol. 3, no. 7, 2012, pp. 1527–34, http:// www. irjabs.com.

[4] Rishi Raj, Prabhat Kumar Sinha, Earnest Vinay Prakash, "Modeling, simulation and analysis of cantilever beam of different material by finite element method, Ansys & MATLAB", *International Journal of Engineering Research and General Science*, vol. 3, no. 3, May-June, 2015, p. 89.

[5] E. Pereira, J. Becedas, I. Payo, F. Ramos, F., V. Feliu, V, "Control of Flexible Manipulators", *Theory and Practice*, Universidad de Costilla-La Mancha, ETS Ingenious Industrials, Ciudad Real, Spain, 2010, pp. 278–9.

[6] S. K. Dwivedy, Peter Eberhard, "Dynamic analysis of flexible manipulators, a literature review," *Mechanism and Machine Theory*, vol. 7, no. 41, 2006, pp. 749–77. DOI: 10.1016/j.mechmachtheory.2006.01.014

[7] S. Ozgoli, H. D. Taghirad, "A Survey on the control of flexible joint robots", (1986-2001), *Asian Journal of Control,* vol. 8, 2006, pp. 1–15. DOI:10.1111/j.1934-6093. 2006.tb00285.x

[8] O.P. Kanna, "Material science and metallurgy," *Dhanpat Rai Publication*, Third Edition, 2009, pp. 23.1–23.31.

[9] S. Ramalingam, S. Rasool Mohideen, et al., "Hybrid polymer composite material for robotic manipulator subject to single link flexibility," *International Journal of Ambient Energy,* 2019. DOI: 10.1080/01430750.2018.1557551

[10] R. Roy, CARIG, Jr., "Structural dynamics and introduction to computer methods," John Wiley, 1981, p. 202. asmedigitalcollection.asme.org.

[11] S. Ramalingam, S. Rasool Mohideen, "Numerical Analysis of Robotic Manipulator Subject to Mechanical Flexibility by Lagrangian Method", *Proc. Natl. Acad. Sci.,* India, Sect. A: Phys. Sci., 2019. doi. org/10.1007/s 40010-019-00619-2

[12] S. Ramalingam, S. Rasool Mohideen, S., "Advanced structural fibre material for single link robotic manipulator simulation analysis with flexibility", *Journal of Automation, Mobile Robotics and Intelligent Systems*, 2019, vol. 13, no. 4, 2019, pp. 38–46. DOI: 10.14313/JAMRIS/4-2019/36

[13] M.O. Tokhi, et al, "Flexible robot manipulators, modeling simulation and control", IET, *Control Engineering Series,* vol. 68, 2008, pp. 23–33. ISBN:978-0-86341-488-0.

[14] Katsuhiko Ogata., *Modern control engineering,* PHI publication, Fifth Edition, 2010, pp. 159–225.

[15] S. Ramalingam, S. Rasool Mohideen, P.S. Sridhar, "Composite material robot manipulator with joint flexibility-Mode and mode shape simulation," *International Journal of Recent Technology and Engineering*, 2019, vol. 8, 4: pp. 902–909, DOI:10.35940/ijrte. D7513.118419

[16] M. Joel Esposito, et. al, "Role of a MATLAB real-time hardware interface within a system modeling course", Proceedings of the 2004 American Society for Engineering Education Annual Conference & Exposition, 2004, P.5.

[17] S. Ramalingam, S. Rasool Mohideen, S. Sounder Rajan, P.S. Sridhar, "Experimental of hybrid polymer composite material robotic single link flexible manipulator", IJITEE, vol.9, no. 3, 2020, pp. 488–494. DOI: 10.35940/ijitee.C8461.019320

[18] Kuldeep Jayaswal, D. K. Palwalia, Suboth Kumar, "Analysis of robust control method for the flexible manipulator in reliable operation of medical robots during COVID-19 pandemic," *Microsystem Technologies*, vol. 27, 2021, pp. 212, 116. DOI: 10.1007/s00542-020-05028-9

[19] Dipendra Subedi, Ilya Tyapin, Geir Hovland, "Review on modeling and control of flexible link manipulators," *Modelling, Identification and Control*, vol. 41, no. 3, 2020, pp. 141–63.

[20] S. Ramalingam, "Dynamic modeling, simulation and analysis of single link robotic manipulator with flexibility", PhD thesis, June 2019, pp. 1034.

[21] Hafiz Muhammad Wahaj Aziz, Jamshed Iqbal, "Flexible Joint Robotic Manipulator: Modeling and Design of Robust Control Law" IEEE, 978-1-5090-4059-9/16, pp. 63–68, 2016. DOI: 10.1109/ICRAI.2016.7791230

[22] Waqar Alam, Nihad Ali, Hafiz Muhammad Wahaj Aziz, Jamshed Iqbal, "Control of flexible joint robotic manipulator: design and prototyping" IEEE, 2018, 978-1-5386-0922-4/18.